1521-0111/105/6/386–394$35.00
MOLECULAR PHARMACOLOGY

dx.doi.org/10.1124/molpharm.123.000818
Mol Pharmacol 105:386–394, June 2024

The M3 Muscarinic Acetylcholine Receptor Can Signal through Multiple G Protein Families[S]

Jeffrey S. Smith, Ari S. Hilibrand, Meredith A. Skiba, Andrew N. Dates, Victor G. Calvillo-Miranda, and Andrew C. Kruse

Department of Biological Chemistry and Molecular Pharmacology, Blavatnik Institute, Harvard Medical School, Boston, Massachusetts (J.S.S., A.S.H., M.A.S., A.N.D., V.G.C.-M., A.C.K.) and Brigham and Women's Hospital, Boston, Massachusetts (J.S.S.)

Received October 23, 2023; accepted April 8, 2024

ABSTRACT

The M3 muscarinic acetylcholine receptor (M_3R) is a G protein–coupled receptor (GPCR) that regulates important physiologic processes, including vascular tone, bronchoconstriction, and insulin secretion. It is expressed on a wide variety of cell types, including pancreatic beta, smooth muscle, neuronal, and immune cells. Agonist binding to the M_3R is thought to initiate intracellular signaling events primarily through the heterotrimeric G protein Gq. However, reports differ on the ability of M_3R to couple to other G proteins beyond Gq. Using members from the four primary G protein families (Gq, Gi, Gs, and G13) in radioligand binding, GTP turnover experiments, and cellular signaling assays, including live cell G protein dissociation and second messenger assessment of cAMP and inositol trisphosphate, we show that other G protein families, particularly Gi and Gs, can also interact with the human M_3R. We further show that these interactions are productive as assessed by amplification of classic second messenger signaling events. Our findings demonstrate that the M_3R is more promiscuous with respect to G protein interactions than previously appreciated.

SIGNIFICANCE STATEMENT

The study reveals that the human M3 muscarinic acetylcholine receptor (M_3R), known for its pivotal roles in diverse physiological processes, not only activates intracellular signaling via Gq as previously known but also functionally interacts with other G protein families such as Gi and Gs, expanding our understanding of its versatility in mediating cellular responses. These findings signify a broader and more complex regulatory network governed by M_3R and have implications for therapeutic targeting.

Introduction

G protein–coupled receptors (GPCRs) are membrane-embedded receptors that regulate nearly every aspect of biology and are among the most successful therapeutic targets across a broad range of diseases. GPCRs initiate signaling through four main families of heterotrimeric G proteins: Gq/11, Gi/o, Gs, and G12/13 (Glukhova et al., 2018). Activated G proteins exchange GDP for GTP on the Gα subunit, dissociating α and obligate dimer βγ subunits. These α and βγ subunits subsequently amplify second messenger signaling cascades. Although each G protein family can induce a variety of downstream effects, the best studied consequences of G protein activation include Gq/11-induced increase in intracellular calcium levels via phospholipase C, DAG, and inositol trisphosphate (IP3); Gs-induced increases in intracellular cAMP; Gi/o-induced decreases intracellular cAMP; and G13-induced regulation of actin polymerization and other cytoskeletal effects (Worzfeld et al., 2008; Newton et al., 2016). Certain GPCRs such as the M_3R are thought to signal primarily through a single Gα protein family, whereas other GPCRs such as the bradykinin and neurokinin-1 receptors are appreciated to signal through multiple G protein families (Liao and Homcy, 1993; Thom et al., 2021; Harris et al., 2022). The G protein:GPCR contact sites thought to convey specificity that are best characterized are the Gα protein C-terminal helical domain interaction with an activated GPCR cytoplasmic pocket (Oldham and Hamm, 2008; Flock et al., 2017). Growing evidence demonstrates that other G protein structural domains as well as the GPCR C terminus and/or intracellular loop 3 as well as

Funding and support were provided by National Institutes of Health National Institute of Arthritis and Musculoskeletal and Skin Diseases Dermatology Training [Grant 5T32AR007098-49] (to J.S.S.), National Cancer Institute [Grant R01CA260415] (to A.C.K.), and National Institute of Child Health and Human Development [Grant 1K99HD110612] (to M.A.S.); the Dermatology Foundation (to J.S.S.); the Fujifilm Fellowship (to A.N.D. and V.G.C.-M.); the Vallee Foundation (to A.C.K.); and the Smith Family Foundation (to A.C.K.).

The authors have declared a conflict of interest. A.C.K. and M.A.S., are coinventors on patent application for AT1R-blocking nanobodies. A.C.K. is a cofounder and consultant for biotechnology companies Tectonic Therapeutic and Seismic Therapeutic and also for the Institute for Protein Innovation, a nonprofit research institute. J.S.S. has received consulting fees from Biogen.

dx.doi.org/10.1124/molpharm.123.000818.

[S] This article has supplemental material available at molpharm.aspetjournals.org.

ABBREVIATIONS: BME, β-mercaptoethanol; BRET, bioluminescence resonance energy transfer; DDM, n-dodecyl-β-D-maltopyranoside; GPCR, G protein–coupled receptor; HBSS, Hanks' balanced salt solution; HEK, human embryonic kidney; IP3, inositol trisphosphate; M_2R, acetylcholine M2 muscarinic receptor; M_3R, acetylcholine M3 muscarinic receptor; NMS, n-methyl-scopolamine; PTX, pertussis toxin; RA, relative activity; TCEP, tris(2-carboxyethyl)phosphine.

membrane phospholipid composition can highly influence G protein:GPCR coupling (Yen et al., 2018; Okashah et al., 2019; Strohman et al., 2019; Heng et al., 2023; Sadler et al., 2023). The relative preference for certain muscarinic receptors for specific G protein pathways appears to be encoded in part through the receptor's second and third intracellular loops (Wess et al., 1990, 1997; Wong and Ross, 1994; Blin et al., 1995).

The M_3R is a well studied rhodopsin-like GPCR that is often considered a model receptor to study Gq-selective signaling. The M_3R is one of the five muscarinic GPCRs (M1–M5) to which acetylcholine binds to initiate cellular responses (Kruse et al., 2014a). For the M_3R, physiologic responses include vasoconstriction, bronchoconstriction, insulin secretion, visual accommodation, and epidermal differentiation (Duttaroy et al., 2004; Kruse et al., 2014b; Duan et al., 2022). The M_3R is expressed in a wide variety of tissues, including smooth muscle and pancreatic beta cells, as well as immune cells such B cells and T cells where their function is not yet clearly established (Kawashima and Fujii, 2004; Wess, 2004). Although the M_3R interaction with the Gq family of G proteins is well supported, its interactions with other G proteins are not firmly established. Certain reports describe interactions with Gi, others with Gs, and still others with neither Gs nor Gi (Peralta et al., 1988; Jones et al., 1991; Inoue et al., 2019; Randáková and Jakubík, 2021; Avet et al., 2022; Sandhu et al., 2022). Prior work has demonstrated incorporation of the stable GTP analog GTPγS or a P32 GTP analog to membranes in both pertussis toxin–sensitive and insensitive manners, strongly suggesting a secondary interaction with Gi that is pertussis toxin sensitive (Lazareno et al., 1993; Offermanns et al., 1994; Akam et al., 2001) However, these and other studies were often limited by the nature of membrane preparations that could contain other muscarinic receptor subtypes, confounding the ability to clearly discern which G protein families were responsible for the observed effects. A more recent study ranks the M_3R with a comparably lower promiscuity index relative to the closely related M_1R, M_2R, and M_4R muscarinic acetylcholine GPCRs as well as comparably lower promiscuity relative to GPCRs with similar levels of available signaling data (Sandhu et al., 2022).

Here we examined if the human M_3R could interact and signal through representative members of the four primary G protein families. We used a variety of methods, including purified protein recombinant systems as well as cellular reporter assays to test our hypothesis. In all, these data demonstrate productive G protein interactions with multiple G protein families, uncovering a previously underappreciated level of promiscuity for this prototypically Gq-coupled GPCR.

Materials and Methods

G Protein Purification. Heterotrimeric G proteins were expressed using a single baculovirus for each human Gα subunit (Gi, Gs, Gq and G13) and a second, bicistronic virus for human Gβ1 and Gγ2-His-tagged subunits in High-Five insect cells similar to previously described (Kruse et al., 2013). For G13α, the first 18 amino acids were replaced with those of Gi1. In brief, insect cells were lysed [10 mM Tris pH 7.5, 10 mM $MgCl_2$, 5 mM β-mercaptoethanol (BME), 10 μM GDP with protease inhibitor and Benzonase]. G proteins were solubilized [20 mM HEPES pH 7.5, 100 mM NaCl, 1% sodium cholate, 0.05% n-dodecyl-β-D-maltopyranoside (DDM), 5 mM $MgCl_2$, 5 mM imidazole, 5 mM BME, 10 μM GDP with protease inhibitor and Benzonase] and eluted from a nickel column (20 mM HEPES pH 7.5, 100 mM NaCl, 0.1% DDM, 1 mM $MgCl_2$, 5 mM BME, 10 μM GDP, 400 mM imidazole). Samples were then dialyzed overnight (20 mM HEPES pH 7.5, 100 mM NaCl, 0.1% DDM, 1 mM $MgCl_2$, 5 mM BME, 20 μM GDP). His tags on Gβ were removed via overnight 3C protease cleavage. Samples were then rerun over a nickel column, and pertinent fractions were treated with lambda phosphatase, calf intestinal phosphatase, and Antarctic phosphatase supplemented with 1 mM manganese chloride for 1 hour on ice. Samples were diluted 1:1 [20 mM HEPES pH 7.4, 0.1% DDM, 1 mM $MgCl_2$, 1 mM tris(2-carboxyethyl)-phosphine (TCEP), 10 μM GDP] followed by ion exchange chromatography and gradient elution (20 mM HEPES pH 7.4, 1 M NaCl, 0.05% DDM, 1 mM $MgCl_2$, 1 mM TCEP, 10 μM GDP). Samples were then concentrated and stored in 20% glycerol at −80°C until use.

M_3R Expression and Purification. N-terminal FLAG-tagged wild-type human M_3R in a pcDNA 3.1 tetracycline/zeocin plasmid (750 μg/l of culture) was transfected into Expi293 cells with a stably integrated tetracycline repressor and grown in Expi293 media (Staus et al., 2018) with FectoPRO (800 μl/l of culture) in the presence of atropine (10 μM). Ten millimolar valproic acid and 1% glucose were added after 18–24 hours. Two days after transfection, cells were induced with 0.4 μg/ml doxycycline and 5 mM sodium butyrate. Cell pellets were harvested 20–26 hours after induction. Frozen cell pellets were resuspended in room-temperature hypotonic lysis buffer (10 mM Tris pH 7.4, 2 mM EDTA, 10 mM $MgCl_2$, 10 μM atropine), with Benzonase nuclease (Sigma-Aldrich) and Pierce protease inhibitor tablets (Thermo Scientific). Cells were pelleted (50,000 × g, 20 minutes) and resuspended in (10 ml/g initial cell pellet) cold solubilization buffer [20 mM HEPES pH 7.4, 750 mM NaCl, 0.5% lauryl maltose neopentyl glycol (LMNG), 0.05% cholesterol hemisuccinate (CHS), 10 mM $MgCl_2$, 10 μM atropine], Benzonase nuclease, Pierce protease inhibitor tablets (Thermo Scientific) and disrupted with a glass Dounce tissue homogenizer. Resuspended lysates were stirred for 2 hours at 4°C. Insoluble material was pelleted by centrifugation (50,000 × g, 30 minutes). The supernatant was filtered through a glass fiber filter, supplemented with 2 mM $CaCl_2$ and passed over M1-αFLAG resin. The resin was washed with 10 column volumes of wash buffer (20 HEPES pH 7.4, 500 mM NaCl, 0.01% LMNG, 0.001% CHS, 2 mM $CaCl_2$, 2 μM atropine) and eluted with elution buffer (20 mM HEPES pH 7.4, 500 mM NaCl, 0.01% LMNG, 0.001% CHS, 1 μM atropine, 5 mM EDTA with 0.2 mg/ml FLAG peptide). The receptor was further purified, and buffer was exchanged by size exclusion chromatography on a Superdex S200 (10/300) column in 20 mM HEPES pH 7.4, 100 mM NaCl, 0.01% LMNG, 0.001% CHS, and 1 μM atropine. Fractions containing the M_3R as assessed through Coomassie gel were pooled and rerun through the same size exclusion chromatography protocol as prior but without atropine. Samples were concentrated and stored at −80°C until use.

Radioligand Binding. Cell membranes for radioligand binding experiments were prepared from 50 ml of a tetracycline-inducible Expi293 cell line as described above and similar to that previously described for other GPCRs (Ahn et al., 2018; Skiba et al., 2023). Cells were pelleted and washed with cold PBS. Cells were resuspended in 2.5 ml of 20 mM Tris pH 7.4 per gram of cell pellet with a protease inhibitor tablet and lysed by Dounce homogenization (100×). Membranes were pelleted by centrifugation at 50,000 × g for 20 minutes and resuspended in 2.5 ml of 50 mM Tris pH 7.4, 12.5 mM $MgCl_2$, 150 mM NaCl, and 0.2% bovine serum albumin (BSA) + protease inhibitor tablet and were Dounce homogenized, flash frozen in liquid nitrogen, and stored at −80°C. After saturation binding experiments confirmed the K_d (Supplemental Fig. 1), membranes were incubated with 1 nM [^{3}H]-N-methyl scopolamine in 50 mM Tris pH 7.4, 12.5 mM $MgCl_2$, 150 mM NaCl, and 0.2% BSA in a 200-μl reaction volume for 120 minutes at room temperature at varying concentrations of cold agonist and with or without the addition of purified G protein at the indicated concentration. Reactions were harvested on a GF/B filter soaked in 0.3% polyethylenimine (Sigma-Aldrich) on a 96-well Brandel harvester and washed three times with cold water. Bound tritium was

extracted overnight with 5 ml scintillation fluid and quantified using a liquid scintillation counter. The counts per minute signal of each block was normalized to the B_{max} of each individual experiment. M_3R levels were calculated at 7.3 pmol/mg protein using saturation binding experiments and the DC Protein Assay (Bio-Rad) according to manufacturer specifications and measuring absorbance at 650 nm.

G Protein Bioluminescence Resonance Energy Transfer TRUPATH Biosensors. TRUPATH integrated plasmids were a gift from Justin English. Assays were conducted similarly to those previously described (Olsen et al., 2020; Eiger et al., 2023). Briefly, human embryonic kidney (HEK) 293T cells were transfected with a human N-terminal FLAG-tagged M_3R in a pcDNA 3.1 expression vector and denoted TRUPATH plasmid. Twenty-four hours later, cells were plated in a 96-well plate in phenol red–free Dulbecco's modified Eagle's medium (DMEM) supplemented with 2% FBS, 1% GlutaMAX, and 1% antibiotic-antimycotic (Sigma). Approximately 48 hours after transfection, media were replaced with assay buffer [Hanks' balanced salt solution (HBSS) without calcium or magnesium + 20 mM HEPES + 3 μM coelenterazine-400a (NanoLight)] and bioluminescence resonance energy transfer (BRET) ratios were obtained using a Promega plate reader.

IP3 Biosensor. IP3 biosensor experiments were conducted similarly to previously described (Inoue et al., 2019). Briefly, HEK293T cells were transfected with the IP3 biosensor expression vector (gift of Asuka Inoue) and a human N-terminal FLAG-tagged M_3R in a pcDNA 3.1 expression vector. Twenty-four hours later, cells were plated in a 96-well plate in phenol red–free DMEM supplemented with 2% FBS, 1% GlutaMAX, and 1% antibiotic-antimycotic (Sigma). Approximately 48 hours after transfection, media were replaced with assay buffer [HBSS without calcium or magnesium + 20 mM HEPES + 3 μM coelenterazine-h (NanoLight)]. Luminescence values were obtained using a Promega plate reader. A preread prior to treatment was conducted, cells were treated with either vehicle or muscarinic agonist, and the plate was subsequently read.

GTP Turnover Assay. The GTP turnover assay was conducted using a modified version of GTPase-Glo assay (Promega), similar to that previously described (Xu et al., 2023). Briefly, purified heterotrimeric G protein was incubated in a 384-well plate with assay buffer consisting of 20 mM HEPES pH 7.4, 0.1% DDM, 100 mM NaCl, 10 mM $MgCl_2$, 5 μM GTP, 5 μM GDP, and 100 μM TCEP with or without 0.125 μM of purified M3R and iperoxo (1 μM) ± tiotropium (2 μM) in a volume of 5 μl, shaking gently at room temperature for 30 minutes. Then, 5 μl of GTPase-Glo reagent (Promega) was added, mixed, and incubated for another 30 minutes at room temperature to convert residual GTP to ATP. Then, 10 μl detection reagent (Promega) was added and incubated for 5–10 minutes, and luminescence was measured using a Promega plate reader. Data were normalized to G protein alone conditions, and statistical analyses were conducted by comparing the effect of M_3R and the agonist iperoxo ± the muscarinic antagonist tiotropium.

GloSensor cAMP Sensor. HEK293T cells were transiently transfected with the human N-terminal FLAG-tagged M_3R in a pcDNA 3.1 expression vector or empty vector control and a modified firefly luciferase (Promega) and transferred to a 96-well plate 24 hours after transfection as previously described (Smith et al., 2017). For pertussis toxin experiments, cells were treated overnight with pertussis toxin (PTX) (200 ng/μl). Approximately 48 hours after transfection, cells were incubated for 2 hours in D-luciferin. Baseline luminescence was measured using a Promega plate reader. Cells were then treated with muscarinic agonist for 10 minutes, and luminescence was again measured.

EPAC cAMP Sensor. HEK293T cells were transiently transfected with the human N-terminal FLAG-tagged M_3R in a pcDNA 3.1 expression vector or empty vector control and the EPAC BRET cAMP biosensor as previously described (Eiger et al., 2022). For pertussis toxin experiments, cells were treated overnight with pertussis toxin (PTX) (200 ng/μl) in plating media. Approximately 48 hours after transfection, the plating media was replaced with assay buffer [HBSS without calcium or magnesium + 20 mM HEPES + 3 μM coelenterazine-h (NanoLight)]. Baseline BRET ratio was measured using a Promega plate reader. Cells were then treated with muscarinic agonist for 10 minutes, and luminescence was again measured. For certain experiments, cells were then treated with isoproterenol (100 nM) for 5 minutes, and luminescence was measured for a third time. For PTX experiments, cells were normalized within their respective baseline conditions (i.e., vehicle or PTX) to account for baseline differences in constitutive Gi signaling caused by PTX prior to maximal signal comparisons.

Bias Factor Calculations. Bias factor calculations were conducted using the intrinsic relative activity model (Rajagopal et al., 2011) as follows: $\beta \pm \Delta\beta$, relative activity (RA) = $(Emax_{Gq} \cdot EC50_{Gi})/(EC50_{Gq} \cdot Emax_{Gi})$ and where $\beta = \log10\ (RA_{\ agonist2}/RA_{\ reference})$. The standard error for this quantity is calculated as follows: $\Delta RA = RA \cdot \sqrt{((\Delta Emax_{Gq}/Emax_{Gq})^2 + (\Delta EC50_{Gq}/EC50_{Gq})^2 + (\Delta Emax_{Gi}/Emax_{Gi})^2 + (\Delta EC50_{Gi}/EC50_{Gi})^2)}$; $\Delta\beta = 0.434\sqrt{(\Delta RA_{agonist2}/RA_{agonist2})^2 + (\Delta RA_{reference}/RA_{reference})^2}$, with Gs interchanged with Gi where appropriate. A calculator is available at https://biasedcalculator.shinyapps.io/calc/ (Smith et al., 2018). The reference agonist was chosen to be carbachol as it has the greatest chemical similarity to the endogenous muscarinic agonist acetylcholine of the three agonists tested throughout this manuscript. Gq was selected as the reference G protein signaling pathway as it is the prototypical cognate G protein for the M_3R.

Statistical Analyses. Statistical analyses were conducted using GraphPad Prism 10. Data are shown as mean ± S.E.M. unless otherwise indicated. For IC_{50} calculations, two log(IC_{50}) site nonlinear regressions were plotted, with IC_{50} values reported for the high-affinity state for Gq, Gi, and Gs (G proteins that displayed a left shift and >10% of estimated pool within the high-affinity state). Conditions without an appreciable high-affinity state were fit with one site Log(IC_{50}) nonlinear regression. Other dose-response curves were calculated by nonlinear regression and three parameter fits (minimum, maximum, and EC_{50}) and were baseline corrected. Details of specific analyses and number of experimental replicates are described within the pertinent methods sections and figure legends, where applicable.

Results

We first examined if agonist binding to the human M_3R was potentiated by purified G protein from the four primary families (Gq, Gi, Gs, and G13) as predicted by the ternary complex model of cooperativity among agonist, GPCR, and effector (e.g., G protein) (De Lean et al., 1980) (Fig. 1A). We performed radioligand competition binding experiments and measured the concentration of a muscarinic agonist required to outcompete a radiolabeled muscarinic antagonist (N-methyl-scopolamine) in the absence or presence of added purified Gq, Gi, Gs, or G13 heterotrimers. Consistent with a functional interaction, Gq, Gs, and Gi changed the IC_{50} and maximal available M_3R to bind antagonist while significantly altering the shape of the competition binding curve, with a rank order change of Gq≫Gi>Gs (Fig. 1B; Table 1). Observed curve shifts occurred in a G protein concentration-dependent manner for Gq (Fig. 1C), Gi (Fig. 1D), and Gs (Fig. 1E). High concentrations of G13 also were able to slightly change the competition binding curve, although this effect was not observed with lower concentrations of purified G13 (Fig. 1F).

We next tested if muscarinic agonists could cause G protein heterotrimer dissociation of Gq, Gs, Gi, and G13 in live cells using TRUPATH biosensors, which use BRET ratios to measure dissociation of Gα-RLuc8 and Gγ-GFP2 (Olsen et al., 2020). BRET-based G protein biosensors and bystander assays have been used for nearly two decades as a measure of

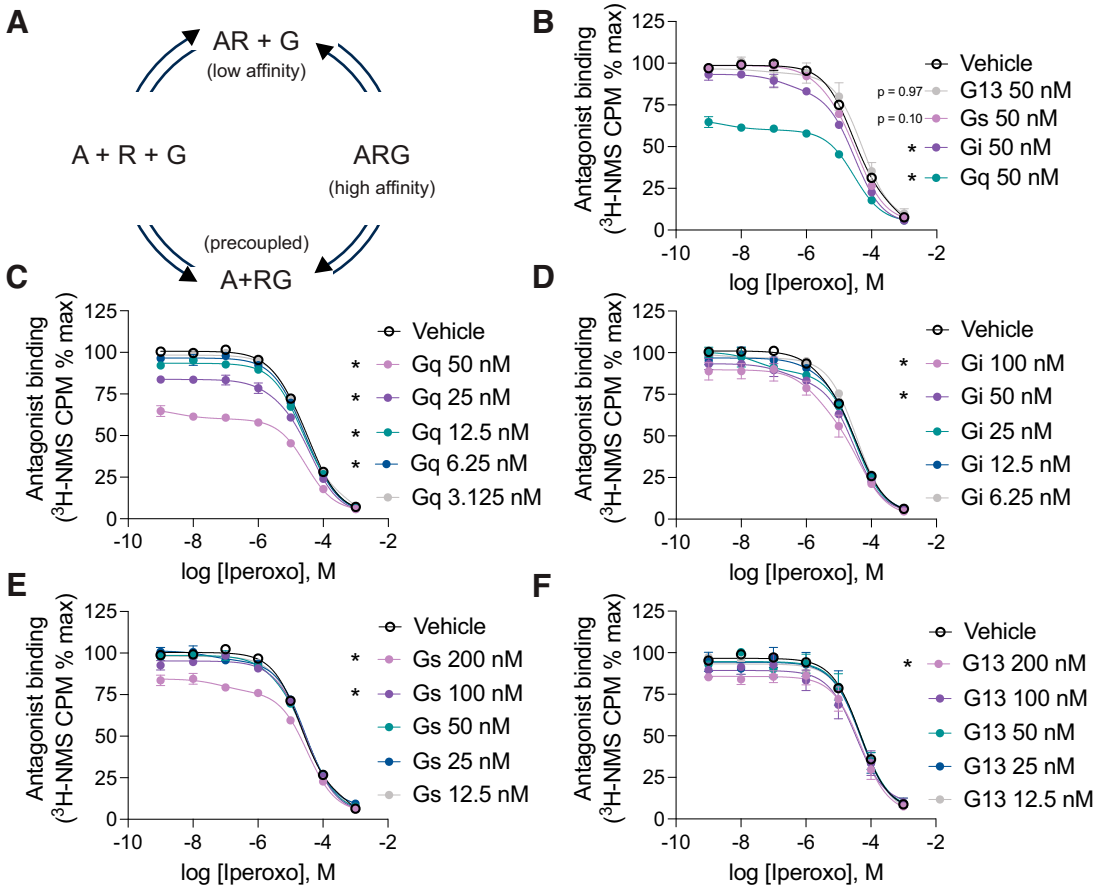

Fig. 1. Purified Gq, Gi, and Gs change M_3R agonist binding profiles. (A) Effector bound receptor has increased affinity for agonists in the ternary complex model. (B) Purified heterotrimer Gq, Gi, Gs, and G13 (50 nM) or vehicle were added to Expi293 cell membranes expressing the M_3R and incubated with the radiolabeled muscarinic antagonist n-methyl-scopolamine (^{3}H-NMS) and competed with varying concentrations of the muscarinic agonist iperoxo. Varying concentrations of (C) purified Gq, (D) purified Gi, (E) purified Gs, or (F) purified G13 heterotrimer in some instances left shifted in the IC_{50} of iperoxo and reduced the available receptor pool available to bind antagonist (lower B_{max}). $N = 3$ independent experiments per condition. Panel A: adapted from (De Lean et al., 1980). Panel B: $^*P < 0.05$, two-way ANOVA, main effect of the indicated G protein relative to vehicle (null hypothesis is that there is no difference from the vehicle condition). Panels C–F: $^*P < 0.05$, two-way ANOVA, Dunnet's post hoc comparison of each respective G protein concentration to vehicle. A, agonist; G, G protein; R, receptor.

G protein activation (Galés et al., 2005, 2006). The absolute magnitude of dissociation (as assessed by change in BRET ratio) relies on multiple properties intrinsic to the biosensor, including expression and relative orientation of the dipole donor to the dipole acceptor, and thus the magnitude of BRET ratio changes cannot be appropriately compared between G protein constructs. We treated cells with three different muscarinic agonists: iperoxo, oxotremorine-M, and carbachol. Carbachol was chosen over the endogenous agonist acetylcholine to avoid possible acetylcholine degradation by acetylcholinesterase. Gq, Gi, and Gs heterotrimers all clearly dissociated after treatment with the three muscarinic agonists in a dose-dependent manner (Fig. 2, A–C; Table 2). Higher concentrations of iperoxo also caused G13 heterotrimer dissociation (Fig. 2D). These responses were M_3R dependent, as cells not overexpressing the M_3R were either minimally able to facilitate TRUPATH biosensor activation (likely through low levels of endogenous muscarinic receptors) or unable to produce appreciable TRUPATH signal (Supplemental Fig. 2). As expected, a prototypical Gi-coupled receptor, the M_2R, and prototypical Gs-coupled, the β-2-adrenergic receptor, also activated the respective TRUPATH biosensors with a greater E_{max} than the M_3R (Supplemental Fig. 3).

TABLE 1

IC_{50} values of data show in Fig. 1B for iperoxo to displace ^{3}H-NMS (1 nM) at the M_3R in the presence of the indicated G protein heterotrimer or vehicle

$N = 3$ replicates per condition for Gq, Gi, Gs, and G13 conditions; $N = 6$ replicates for vehicle condition.

	Log(IC_{50})	Standard Error
Gq	−8.5	1.2
Gi	−6.7	0.79
Gs	−5.5	0.51
G13	−4.3	0.12
Vehicle	−4.5	0.05

A critical component of G protein activation is exchange of GDP for GTP on the G protein α subunit. G protein nucleotide exchange is expedited by guanine nucleotide exchange factors, which include GPCRs. Activated G proteins eventually hydrolyze GTP independently (in vivo, this is augmented by GTPases), which terminates canonical G protein activation and promotes reassociation of the G protein heterotrimer in the GDP bound state (Dror et al., 2015). We measured nucleotide exchange through the GTP-Glo assay, which measures GTP hydrolysis, in a recombinant system consisting of purified G protein in the presence or absence of purified full-length M_3

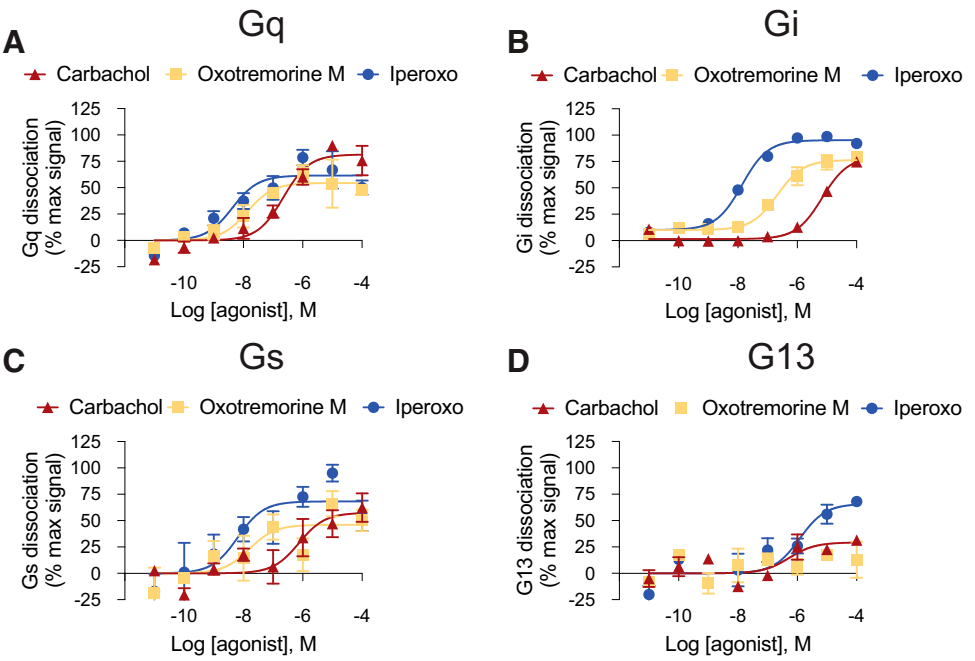

Fig. 2. M_3R-mediated G protein dissociation. HEK293T cells were transiently transfected with the M_3R and the indicated integrated TRUPATH BRET construct. Cells were treated with the indicated muscarinic agonist and measured ~2 minutes later for (A) Gq, (B) Gi, (C) Gs, and (D) G13 dissociation of G protein β and $\beta\gamma$ subunits. N = 3–5 independent experiments per condition.

R in detergent and the agonist iperoxo. Size exclusion chromatography traces (Fig. 3A) with specific radioligand binding to the purified protein confirmed the functionality of full-length M_3R used in these assays (Fig. 3B). As the intrinsic GTPase activity differs between G protein families, intrinsic levels of GTP hydrolysis at each G protein were empirically determined so that similar levels of basal hydrolysis occurred in the G protein alone condition (Supplemental Fig. 4). Purified M_3R facilitated GTP consumption with three of the four families of G protein, with G13 not statistically different (P = 0.20). Pretreatment with the pseudo-irreversible muscarinic antagonist tiotropium reversed this effect (Fig. 3, C–F).

We then confirmed that the activated Gs, Gi, and Gq facilitated M_3R second messenger amplification upon agonist treatment. As expected, M_3R agonists increased intracellular IP3 levels (Fig. 4, A and B) in biosensor measurements in live cells. We further examined if the M_3R propagates signals through Gs and Gi by examining intracellular cAMP levels. Using a previously validated BRET-based EPAC cAMP biosensor (Fig. 5A), we observed that muscarinic agonist treatment of cells expressing M_3R caused an increase in intracellular cAMP, consistent with Gs pathway activity (Fig. 5B). Pertussis toxin pretreatment revealed a further increase in cAMP, suggesting competing Gi signaling that dampened adenyl cyclase activity (Fig. 5C). The inhibitory component of M_3R-mediated cAMP signaling was additionally unmasked by treating cells with the β-adrenergic agonist isoproterenol, which elevated global cAMP in all conditions but to a lesser degree in conditions treated with M_3R agonists (Fig. 5D). We also observed Gs- and Gi-mediated effects on cAMP levels by the M_3R using the GloSensor assay, an orthogonal approach to measuring cAMP production. In this assay, pertussis toxin also revealed both Gs and Gi signaling contributions (Supplemental Fig. 5). These effects were M_3R dependent, as cells transfected with empty vector as opposed to M_3R vector showed no significant effect of muscarinic agonist (Supplemental Fig. 5).

Discussion

The M_3R often serves as a model GPCR for Gq-selective signaling responses. Here, using three muscarinic agonists, we demonstrate that other G protein families can also functionally interact with the M_3R and activate canonical second messenger signaling pathways. From the data collected in this study, a relatively preserved rank order of Gq≫Gi>Gs>G13 across assays was observed, although in vivo functional rank order is likely to be determined by G protein expression differences, which can vary dramatically between cell and tissue types (Wilkie et al., 1991; El-Haibi et al., 2013). We demonstrate functional G protein association to the M_3R in a variety of assays, including radioligand binding, purified protein, and multiple signaling assays in live cells.

One of these assays, TRUPATH, relies upon artificial BRET tags to detect signal. Recent studies by Inoue et al. (2019) and Avet et al. (2022) use similar biosensor technology to measure G protein activation, although in the Avet study only Gs alpha

TABLE 2
EC_{50} values of TRUPATH data shown in Fig. 2 for three different M_3R agonists

	Log(EC_{50}) Carbachol	Standard Error	Log(EC_{50}) Oxotremorine-M	Standard Error	Log(EC_{50}) Iperoxo	Standard Error
Gq	−6.7	0.21	−7.9	0.34	−8.4	0.34
Gi	−5.2	0.10	−6.7	0.14	−7.9	0.08
Gs	−6.1	0.43	−7.8	0.64	−8.2	0.46
G13	−6.2	0.53	Poor fit	—	−5.9	0.31

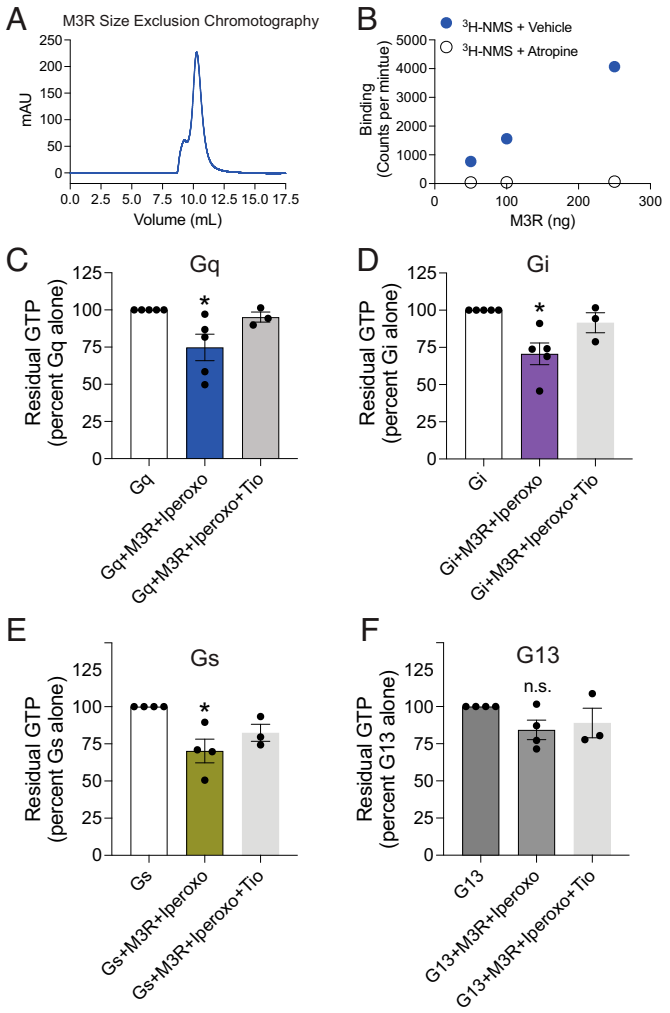

Fig. 3. M_3R-facilitated GTP turnover in four G protein families. (A) Size exclusion chromatography trace of purified M_3R. (B) Specific (vehicle-treated) and nonspecific (atropine-treated) binding of the radiolabeled muscarinic antagonist n-methyl-scopolamine (^{3}H-NMS) to purified M_3R. Residual GTP normalized to basal intrinsic G protein GTP hydrolysis with the M_3R and (C) purified Gq, (D) purified Gi, (E) purified Gs, or (F) purified G13. N = 3–5 independent experiments per condition, $^*P <$ 0.05, one-way ANOVA with Dunnett's post hoc comparison with the G protein without receptor condition. Tio, muscarinic antagonist tiotropium (2 μM).

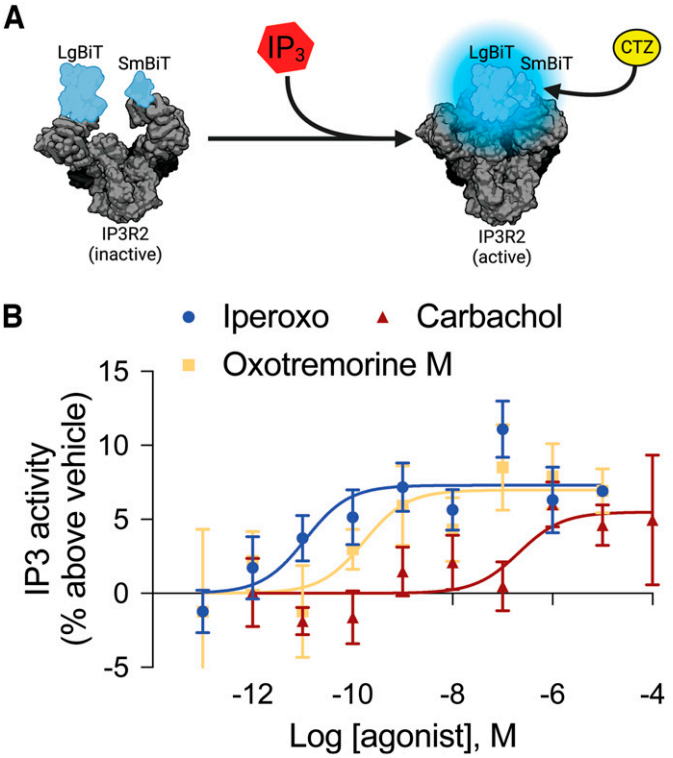

Fig. 4. M_3R agonists expectedly increase intracellular IP3 (A) schematic of a previously validated Gq-dependent IP3 biosensor designed by Inoue and colleagues. (B) IP3 biosensor and the M_3R were transiently transfected in HEK293T cells and treated with the indicated agonist demonstrating an increase in IP3 activity. N = 8 independent experiments per condition. Panel A created with BioRender.com.

required direct G protein subunit labeling. Our TRUPATH findings (Fig. 2) align with these findings for both Gq and Gi, and our biochemical data using untagged, purified protein provides further support to these cellular observations. Similarly, Ilyaskina and colleagues (2018) observed an approximate 10-fold difference in M_3R interaction with Gq (higher association) and Go (lower association) using fluorescence resonance energy transfer (FRET)-based approaches. However, they did not report a notable interaction signal with Gs or G13. Different muscarinic agonists used and distinct methods likely explain the differences in Gs activity observations. Our findings build upon these prior studies by also observing Gs TRUPATH activity downstream of the M_3R, similarly supported by our biochemical assays and cellular second messenger cAMP assays.

Native G proteins in the HEK293 were present in our experimental conditions. Although competition for different G protein families by a given receptor is expected in the dynamic native conditions of a normal cellular environment, it is reassuring that Avet and colleagues (2022) reported that competition with endogenous G proteins did not occur to a notable extent when compared with similar experiments conducted in cells lacking the different G protein family members by genetic deletion. Some prior studies have not necessarily observed the same level of G protein promiscuity that we report here (Sandhu et al., 2022). This may be in part because some current G protein assays rely on heavily modified G proteins [e.g., mini–G proteins (Carpenter et al., 2016) (which often share a Gs backbone) or assays where only the alpha-5 helix of the G protein, known to be necessary for GPCR core interactions to facilitate nucleotide exchange, are altered] (Inoue et al., 2012). Although these tools have been very useful to the field and facilitated structural advances and large screening studies, such alternations may contribute to the seemingly discrepant results. Comparison of Avet and Inoue's recent data sets reveal 64% identity of couplings between the effector membrane translocation assays and Inoue's 2019 data set, highlighting the importance of orthogonal experimental approaches that complement existing studies in determining the GPCR coupling profile of a given receptor (Inoue et al., 2019; Avet et al., 2022). Currently, the structural features that encode family selectivity between GPCRs and G proteins are still not well understood and remain an area of active research; however, it is appreciated that critical contacts exist between GPCRs and G proteins beyond the alpha-5 helix and receptor core (Yen et al., 2018; Okashah et al., 2019; Strohman et al., 2019; Heng et al., 2023; Sadler et al., 2023). The subcellular

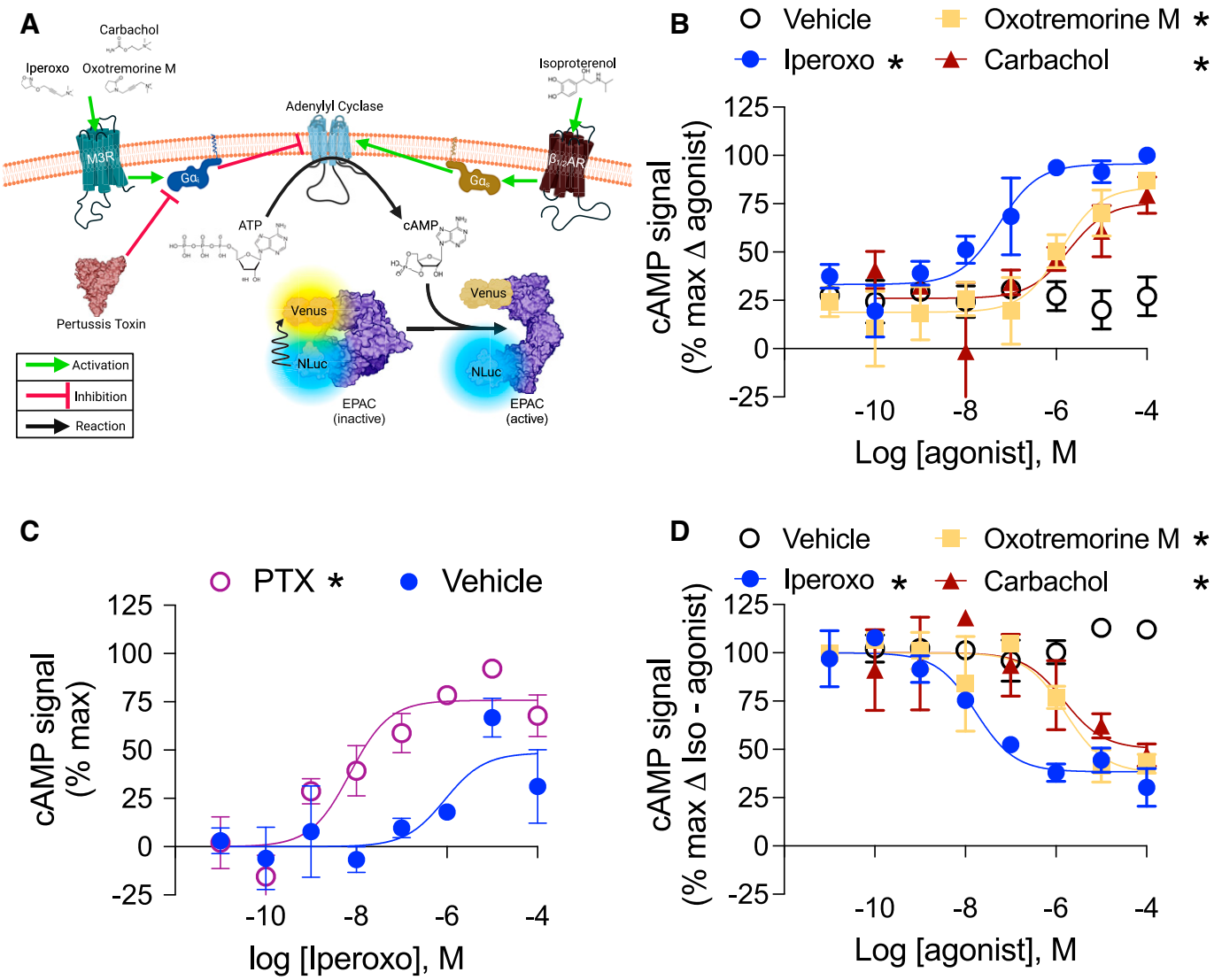

Fig. 5. Unmasking Gi contribution of M_3R agonists. (A) Diagram of BRET EPAC cAMP biosensor. HEK293T cells were transiently transfected with the cAMP biosensor and the M_3R. (B) Cells were treated for 10 minutes with the indicated agonist and measured for cAMP signal. (C) Cells were pretreated with pertussis toxin and cAMP signal was assessed after treatment with iperoxo, which resulted in a left-shifted EC_{50} and an increased E_{max}. (D) After agonist treatment, cells were treated with isoproterenol (100 nM) for 5 minutes, with cells previously treated with an M_3R agonist showing reduced cAMP signal. $N = 3$ independent experiments per condition. *$P < 0.05$ by two-way ANOVA, main effect of the indicated agonist versus vehicle (null hypothesis is that there is no difference from the vehicle condition). Panel A created with BioRender.com.

compartment where a G protein interacts with a GPCR is known to influence biologic responses (Irannejad et al., 2017; Eiger et al., 2022; Kwon et al., 2022; Lin et al., 2023) and may also refine G protein:GPCR pairings.

As different ligands for the same receptor can initiate distinct intracellular signaling events, a term referred to as biased signaling, we tested three established agonists in our signaling assays. The relative rank order of potency of iperoxo->oxotremorine-M>carbachol was preserved in both G protein and second messenger signaling experiments in live cells. Iperoxo displayed numerical bias for Gi over Gq pathways, although this was not statistically significant (Supplemental Fig. 6). Further work with these and other muscarinic agonists may uncover preferences for certain agonists for specific muscarinic secondary G protein pathways. Gq clearly couples most efficiently to the M_3R, as expected. The addition of purified Gq caused the greatest left shift in IC_{50} in radioligand competition binding experiments compared with the more modest IC_{50} left shifts caused by the addition of Gi or Gs. Nevertheless, the M_3R interacts with Gi and Gs at concentrations in both purified protein conditions and in live cells that are reasonably expected to be physiologically relevant, as the relative distribution of GPCRs and G proteins on the plasma membrane are not equally distributed and found to be colocalized to 'hotspots' (Sungkaworn et al., 2017). In certain experiments, G13 also had evidence of M_3R-mediated activity, although consistent G13 responses across experiments were not observed.

Given that the relative level of G proteins within cell types appears to vary considerably depending on the tissue identity and disease state, nonprimary and lower-affinity receptor G protein interactions could be biologically relevant in certain physiologic contexts. Such 'systems bias,' where signaling events between cell types differ due to levels of intracellular effectors like G proteins, could alter the expected effects of a therapeutic or lead to unintended effects (Smith et al., 2018).

Thus, it is possible in certain cell types or tissues that non-Gq G proteins are the principal G protein effectors of the M_3R. Further work is necessary to test this hypothesis.

A limitation of our work in cells is that the experiments rely on overexpressed conditions or purified M_3R. It is possible that the observed G protein coupling promiscuity is most pronounced when M_3R levels are high or in cells where certain G proteins are low or absent. Nevertheless, overexpressed conditions and purified protein have historically provided useful models that are often translatable to the true physiology. Like G proteins, expression of the M_3R can vary substantially between cell types and disease status (Shi et al., 2004). We do not claim that the M_3R predominately signals through non-Gq–related proteins under all, or even the majority, of conditions. Rather, we report that the M_3R, a prototypical Gq-coupled receptor, is more promiscuous with respect to G proteins than widely appreciated. We suspect that other GPCRs will show similar, more nuanced functional G protein pairings.

Acknowledgments

The authors thank Justin English for sharing TRUPATH constructs, Asuka Inoue for sharing the IP3 biosensor, Stephen Blacklow for use of laboratory equipment and resources, and Biswaranjan Pani and Laura Wingler for helpful discussions.

Data Availability

The authors declare that all of the data supporting the findings of this study are available within the paper and its Supplemental Material.

Authorship Contributions

Participated in research design: Smith, Skiba, Calvillo-Miranda, Kruse.

Conducted experiments: Smith, Hilibrand.

Contributed new reagents or analytic tools: Dates.

Performed data analysis: Smith, Hilibrand.

Wrote or contributed to the writing of the manuscript: Smith, Kruse.

References

Ahn S, Pani B, Kahsai AW, Olsen EK, Husemoen G, Vestergaard M, Jin L, Zhao S, Wingler LM, Rambarat PK, et al. (2018) Small-molecule positive allosteric modulators of the β_2-adrenoceptor isolated from DNA-encoded libraries. *Mol Pharmacol* **94**:850–861.

Akam EC, Challiss RA, and Nahorski SR (2001) G(q/11) and G(i/o) activation profiles in CHO cells expressing human muscarinic acetylcholine receptors: dependence on agonist as well as receptor-subtype. *Br J Pharmacol* **132**:950–958.

Avet C, Mancini A, Breton B, Le Gouill C, Hauser AS, Normand C, Kobayashi H, Gross F, Hogue M, Lukasheva V, et al. (2022) Effector membrane translocation biosensors reveal G protein and βarrestin coupling profiles of 100 therapeutically relevant GPCRs. *eLife* **11**:e74101.

Blin N, Yun J, and Wess J (1995) Mapping of single amino acid residues required for selective activation of Gq/11 by the m3 muscarinic acetylcholine receptor. *J Biol Chem* **270**:17741–17748.

Carpenter B, Nehmé R, Warne T, Leslie AG, and Tate CG (2016) Structure of the adenosine A(2A) receptor bound to an engineered G protein. *Nature* **536**:104–107.

De Lean A, Stadel JM, and Lefkowitz RJ (1980) A ternary complex model explains the agonist-specific binding properties of the adenylate cyclase-coupled beta-adrenergic receptor. *J Biol Chem* **255**:7108–7117.

Dror RO, Mildorf TJ, Hilger D, Manglik A, Borhani DW, Arlow DH, Philippsen A, Villanueva N, Yang Z, Lerch MT, et al. (2015) SIGNAL TRANSDUCTION. Structural basis for nucleotide exchange in heterotrimeric G proteins. *Science* **348**:1361–1365.

Duan J, Grando C, Liu S, Chernyavsky A, Chen JK, Andersen B, and Grando SA (2022) The M3 muscarinic acetylcholine receptor promotes epidermal differentiation. *J Invest Dermatol* **142**:3211–3221.e2.

Duttaroy A, Zimliki CL, Gautam D, Cui Y, Mears D, and Wess J (2004) Muscarinic stimulation of pancreatic insulin and glucagon release is abolished in m3 muscarinic acetylcholine receptor-deficient mice. *Diabetes* **53**:1714–1720.

Eiger DS, Boldizsar N, Honeycutt CC, Gardner J, Kirchner S, Hicks C, Choi I, Pham U, Zheng K, Warman A, et al. (2022) Location bias contributes to functionally selective responses of biased CXCR3 agonists. *Nat Commun* **13**:5846.

Eiger DS, Smith JS, Shi T, Stepniewski TM, Tsai CF, Honeycutt C, Boldizsar N, Gardner J, Nicora CD, Moghieb AM, et al. (2023) Phosphorylation barcodes direct biased chemokine signaling at CXCR3. *Cell Chem Biol* **30**:362–382.e8.

El-Haibi CP, Sharma P, Singh R, Gupta P, Taub DD, Singh S, and Lillard Jr JW (2013) Differential G protein subunit expression by prostate cancer cells and their interaction with CXCR5. *Mol Cancer* **12**:64.

Flock T, Hauser AS, Lund N, Gloriam DE, Balaji S, and Babu MM (2017) Selectivity determinants of GPCR-G-protein binding. *Nature* **545**:317–322.

Galés C, Rebois RV, Hogue M, Trieu P, Breit A, Hébert TE, and Bouvier M (2005) Real-time monitoring of receptor and G-protein interactions in living cells. *Nat Methods* **2**:177–184.

Galés C, Van Durm JJ, Schaak S, Pontier S, Percherancier Y, Audet M, Paris H, and Bouvier M (2006) Probing the activation-promoted structural rearrangements in preassembled receptor-G protein complexes. *Nat Struct Mol Biol* **13**:778–786.

Glukhova A, Draper-Joyce CJ, Sunahara RK, Christopoulos A, Wootten D, and Sexton PM (2018) Rules of engagement: GPCRs and G proteins. *ACS Pharmacol Transl Sci* **1**:73–83.

Harris JA, Faust B, Gondin AB, Dämgen MA, Suomivuori CM, Veldhuis NA, Cheng Y, Dror RO, Thal DM, and Manglik A (2022) Selective G protein signaling driven by substance P-neurokinin receptor dynamics. *Nat Chem Biol* **18**:109–115.

Heng J, Hu Y, Pérez-Hernández G, Inoue A, Zhao J, Ma X, Sun X, Kawakami K, Ikuta T, Ding J, et al. (2023) Function and dynamics of the intrinsically disordered carboxyl terminus of β2 adrenergic receptor. *Nat Commun* **14**:2005.

Ilyaskina OS, Lemoine H, and Bünemann M (2018) Lifetime of muscarinic receptor-G-protein complexes determines coupling efficiency and G-protein subtype selectivity. *Proc Natl Acad Sci USA* **115**:5016–5021.

Inoue A, Ishiguro J, Kitamura H, Arima N, Okutani M, Shuto A, Higashiyama S, Ohwada T, Arai H, Makide K, et al. (2012) TGFα shedding assay: an accurate and versatile method for detecting GPCR activation. *Nat Methods* **9**:1021–1029.

Inoue A, Raimondi F, Kadji FMN, Singh G, Kishi T, Uwamizu A, Ono Y, Shinjo Y, Ishida S, Arang N, et al. (2019) Illuminating G-protein-coupling selectivity of GPCRs. *Cell* **177**:1933–1947.e25.

Irannejad R, Pessino V, Mika D, Huang B, Wedegaertner PB, Conti M, and von Zastrow M (2017) Functional selectivity of GPCR-directed drug action through location bias. *Nat Chem Biol* **13**:799–806.

Jones SV, Heilman CJ, and Brann MR (1991) Functional responses of cloned muscarinic receptors expressed in CHO-K1 cells. *Mol Pharmacol* **40**:242–247.

Kawashima K and Fujii T (2004) Expression of non-neuronal acetylcholine in lymphocytes and its contribution to the regulation of immune function. *Front Biosci* **9**:2063–2085.

Kruse AC, Kobilka BK, Gautam D, Sexton PM, Christopoulos A, and Wess J (2014a) Muscarinic acetylcholine receptors: novel opportunities for drug development. *Nat Rev Drug Discov* **13**:549–560.

Kruse AC, Li J, Hu J, Kobilka BK, and Wess J (2014b) Novel insights into M3 muscarinic acetylcholine receptor physiology and structure. *J Mol Neurosci* **53**:316–323.

Kruse AC, Ring AM, Manglik A, Hu J, Hu K, Eitel K, Hübner H, Pardon E, Valant C, Sexton PM, et al. (2013) Activation and allosteric modulation of a muscarinic acetylcholine receptor. *Nature* **504**:101–106.

Kwon Y, Mehta S, Clark M, Walters G, Zhong Y, Lee HN, Sunahara RK, and Zhang J (2022) Non-canonical β-adrenergic activation of ERK at endosomes. *Nature* **611**:173–179.

Lazareno S, Farries T, and Birdsall NJ (1993) Pharmacological characterization of guanine nucleotide exchange reactions in membranes from CHO cells stably transfected with human muscarinic receptors m1-m4. *Life Sci* **52**:449–456.

Liao JK and Homcy CJ (1993) The G proteins of the G alpha i and G alpha q family couple the bradykinin receptor to the release of endothelium-derived relaxing factor. *J Clin Invest* **92**:2168–2172.

Lin T-Y, Mai QN, Zhang H, Wilson E, Chien H-C, Yee SW, Giacomini KM, Olgin JE, and Irannejad R, (2023) Cardiac contraction and relaxation are regulated by distinct subcellular cAMP pools. *Nat Chem Biol* **20**:62–73.

Newton AC, Bootman MD, and Scott JD (2016) Second messengers. *Cold Spring Harb Perspect Biol* **8**:a005926.

Offermanns S, Wieland T, Homann D, Sandmann J, Bombien E, Spicher K, Schultz G, and Jakobs KH (1994) Transfected muscarinic acetylcholine receptors selectively couple to Gi-type G proteins and Gq/11. *Mol Pharmacol* **45**:890–898.

Okashah N, Wan Q, Ghosh S, Sandhu M, Inoue A, Vaidehi N, and Lambert NA (2019) Variable G protein determinants of GPCR coupling selectivity. *Proc Natl Acad Sci USA* **116**:12054–12059.

Oldham WM and Hamm HE (2008) Heterotrimeric G protein activation by G-protein-coupled receptors. *Nat Rev Mol Cell Biol* **9**:60–71.

Olsen RHJ, DiBerto JF, English JG, Glaudin AM, Krumm BE, Slocum ST, Che T, Gavin AC, McCorvy JD, Roth BL, et al. (2020) TRUPATH, an open-source biosensor platform for interrogating the GPCR transducerome. *Nat Chem Biol* **16**:841–849.

Peralta EG, Ashkenazi A, Winslow JW, Ramachandran J, and Capon DJ (1988) Differential regulation of PI hydrolysis and adenylyl cyclase by muscarinic receptor subtypes. *Nature* **334**:434–437.

Rajagopal S, Ahn S, Rominger DH, Gowen-MacDonald W, Lam CM, Dewire SM, Violin JD, and Lefkowitz RJ (2011) Quantifying ligand bias at seven-transmembrane receptors. *Mol Pharmacol* **80**:367–377.

Randáková A and Jakubík J (2021) Functionally selective and biased agonists of muscarinic receptors. *Pharmacol Res* **169**:105641.

Sadler F, Ma N, Ritt M, Sharma Y, Vaidehi N, and Sivaramakrishnan S (2023) Autoregulation of GPCR signalling through the third intracellular loop. *Nature* **615**:734–741.

Sandhu M, Cho A, Ma N, Mukhaleva E, Namkung Y, Lee S, Ghosh S, Lee JH, Gloriam DE, Laporte SA, et al. (2022) Dynamic spatiotemporal determinants modulate GPCR:G protein coupling selectivity and promiscuity. *Nat Commun* **13**:7428.

Shi H, Wang H, Li D, Nattel S, and Wang Z (2004) Differential alterations of receptor densities of three muscarinic acetylcholine receptor subtypes and current densities

of the corresponding K+ channels in canine atria with atrial fibrillation induced by experimental congestive heart failure. *Cell Physiol Biochem* **14**:31–40.
Skiba MA, Sterling SM, Rawson S, Gilman MSA, Xu H, Nemeth GR, Hurley JD, Shen P, Status DP, Kim J, et al. (2023) Antibodies expand the scope of angiotensin receptor pharmacology. *bioRxiv* DOI: 10.1101/2023.08.23.554128
Smith JS, Alagesan P, Desai NK, Pack TF, Wu JH, Inoue A, Freedman NJ, and Rajagopal S (2017) C-X-C motif chemokine receptor 3 splice variants differentially activate beta-arrestins to regulate downstream signaling pathways. *Mol Pharmacol* **92**:136–150.
Smith JS, Lefkowitz RJ, and Rajagopal S (2018) Biased signalling: from simple switches to allosteric microprocessors. *Nat Rev Drug Discov* **17**:243–260.
Staus DP, Wingler LM, Choi M, Pani B, Manglik A, Kruse AC, and Lefkowitz RJ (2018) Sortase ligation enables homogeneous GPCR phosphorylation to reveal diversity in β-arrestin coupling. *Proc Natl Acad Sci USA* **115**:3834–3839.
Strohman MJ, Maeda S, Hilger D, Masureel M, Du Y, and Kobilka BK (2019) Local membrane charge regulates β_2 adrenergic receptor coupling to G_{i3}. *Nat Commun* **10**:2234.
Sungkaworn T, Jobin ML, Burnecki K, Weron A, Lohse MJ, and Calebiro D (2017) Single-molecule imaging reveals receptor-G protein interactions at cell surface hot spots. *Nature* **550**:543–547.
Thom C, Ehrenmann J, Vacca S, Waltenspühl Y, Schöppe J, Medalia O, and Plückthun A (2021) Structures of neurokinin 1 receptor in complex with G_q and G_s proteins reveal substance P binding mode and unique activation features. *Sci Adv* **7**:eabk2872.
Wess J (2004) Muscarinic acetylcholine receptor knockout mice: novel phenotypes and clinical implications. *Annu Rev Pharmacol Toxicol* **44**:423–450.
Wess J, Bonner TI, and Brann MR (1990) Chimeric m2/m3 muscarinic receptors: role of carboxyl terminal receptor domains in selectivity of ligand binding and coupling to phosphoinositide hydrolysis. *Mol Pharmacol* **38**:872–877.
Wess J, Liu J, Blin N, Yun J, Lerche C, and Kostenis E (1997) Structural basis of receptor/G protein coupling selectivity studied with muscarinic receptors as model systems. *Life Sci* **60**:1007–1014.
Wilkie TM, Scherle PA, Strathmann MP, Slepak VZ, and Simon MI (1991) Characterization of G-protein alpha subunits in the Gq class: expression in murine tissues and in stromal and hematopoietic cell lines. *Proc Natl Acad Sci USA* **88**:10049–10053.
Wong SK and Ross EM (1994) Chimeric muscarinic cholinergic:beta-adrenergic receptors that are functionally promiscuous among G proteins. *J Biol Chem* **269**:18968–18976.
Worzfeld T, Wettschureck N, and Offermanns S (2008) G(12)/G(13)-mediated signalling in mammalian physiology and disease. *Trends Pharmacol Sci* **29**:582–589.
Xu J, Wang Q, Hübner H, Hu Y, Niu X, Wang H, Maeda S, Inoue A, Tao Y, Gmeiner P, et al. (2023) Structural and dynamic insights into supra-physiological activation and allosteric modulation of a muscarinic acetylcholine receptor. *Nat Commun* **14**:376.
Yen HY, Hoi KK, Liko I, Hedger G, Horrell MR, Song W, Wu D, Heine P, Warne T, Lee Y, et al. (2018) $PtdIns(4,5)P_2$ stabilizes active states of GPCRs and enhances selectivity of G-protein coupling. *Nature* **559**:423–427.

Address correspondence to: Dr. Andrew C. Kruse, Harvard Medical School, Seeley G. Mudd Building Room 232A, 250 Longwood Avenue, Boston, MA 02115. E-mail: andrew_kruse@hms.harvard.edu

The M3 muscarinic acetylcholine receptor can signal through multiple G protein families

Jeffrey S. Smith, Ari S. Hilibrand, Meredith A. Skiba, Andrew N. Dates, Victor G. Calvillo-Miranda, and Andrew C. Kruse

MOLPHARM-AR-2023-000818

Supplementary figures

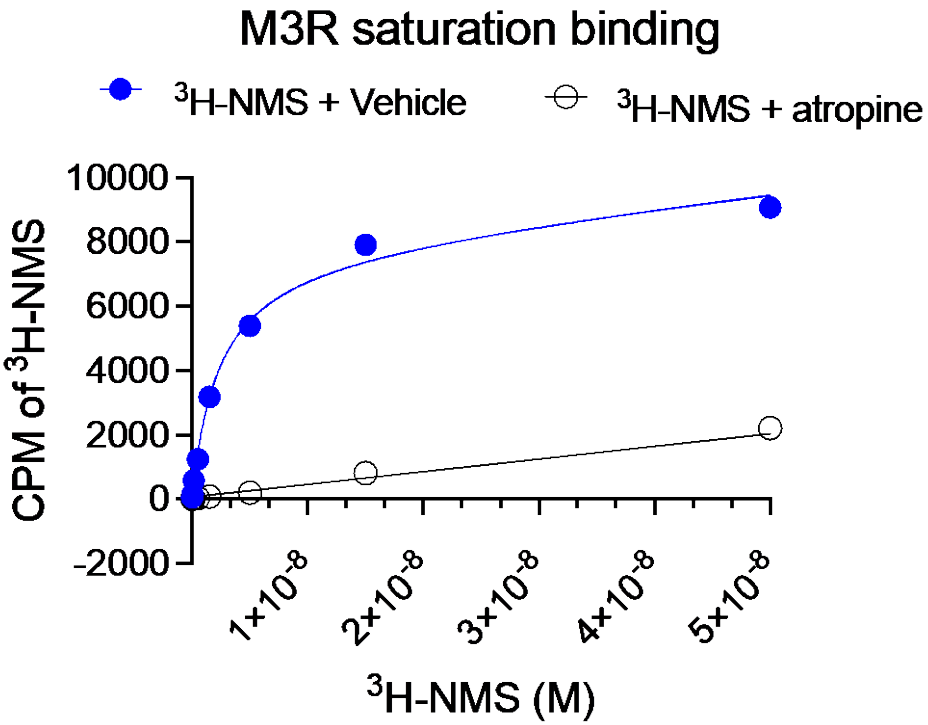

Supplemental Figure 1: Saturation binding of tritiated N-methyl-scopolamine in Expi 293 cell membranes expressing the M_3R to determine concentration of antagonist to use in competition binding assays (Figure 1). Specific (blue, vehicle) and non-specific (clear, muscarinic antagonist atropine (1 μM)) were compared to calculate the Kd (2.3 nM). Samples were run in triplicate.

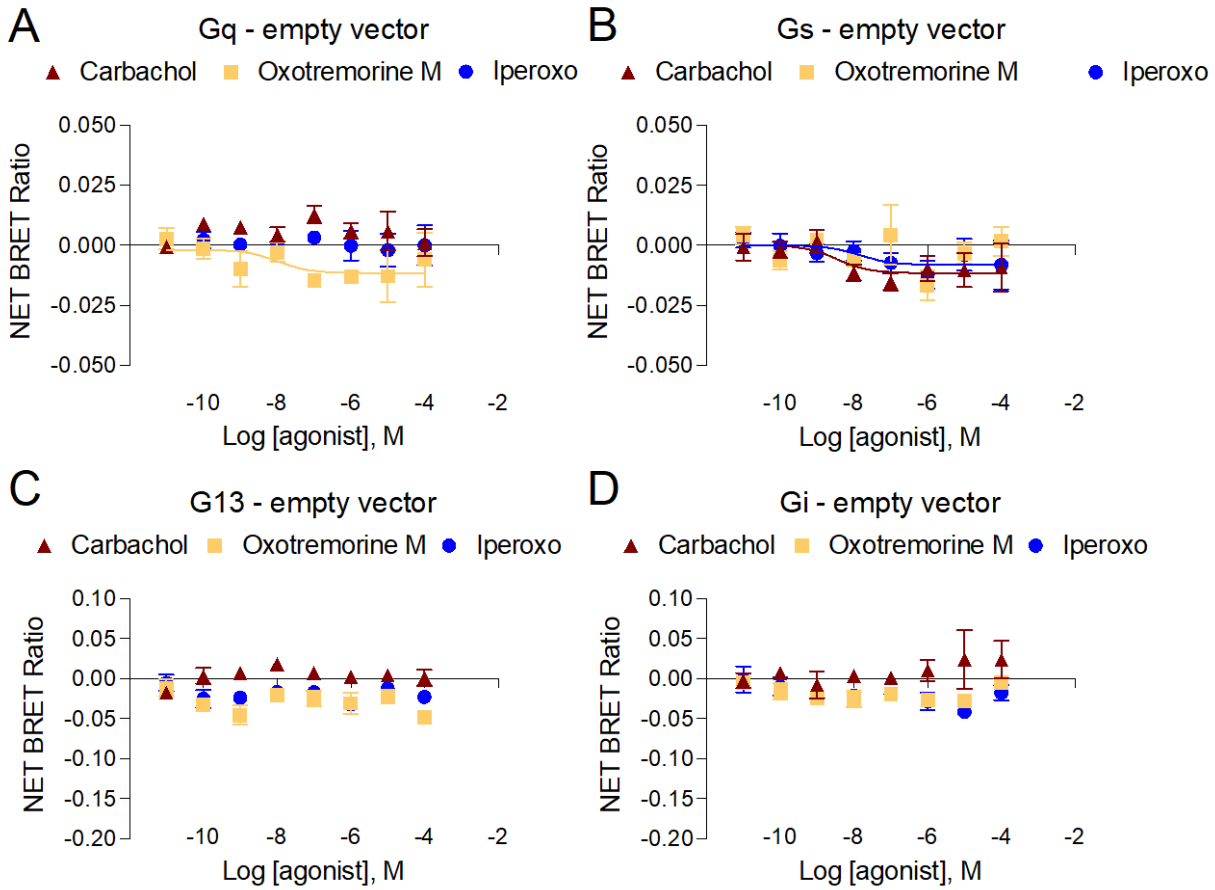

Supplemental Figure 2: Empty vector control (in place of M_3R) in TRUPATH assays. HEK 293T cells were transiently transfected with the indicated TRUPATH integrated construct and pcDNA empty vector control. (A) Minimal Gq dissociation was observed in response to oxotremorine M. (B) Minimal Gs signal was observed in response to agonist treatment. (C) No consistent G13 and (D) no consistent Gi signal were observed. n=3-4 per condition.

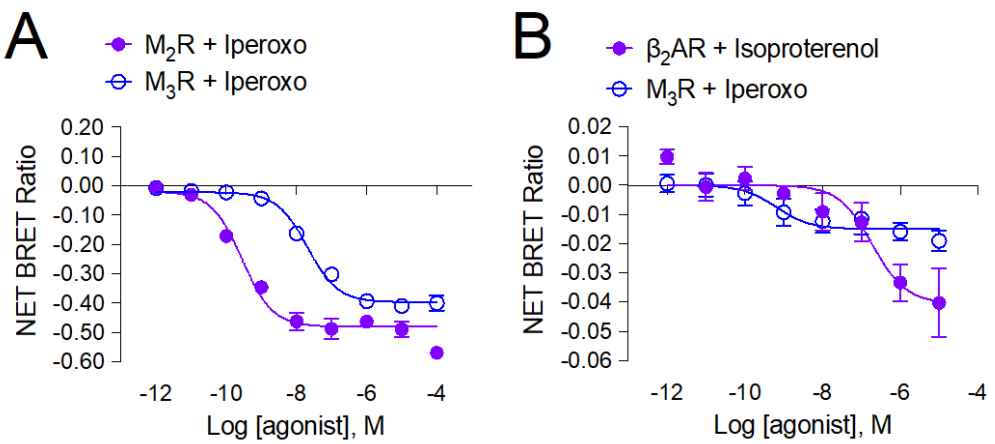

Supplemental Figure 3: Comparison of (A) Gi TRUPATH dose-response with a prototypical Gi-coupled receptor, M_2R and (B) Gs TRUPATH dose-response with a prototypical Gs-coupled receptor, β-2-adrenergic receptor (β_2AR). For panel A, N=4-7; for panel B, N=3-8.

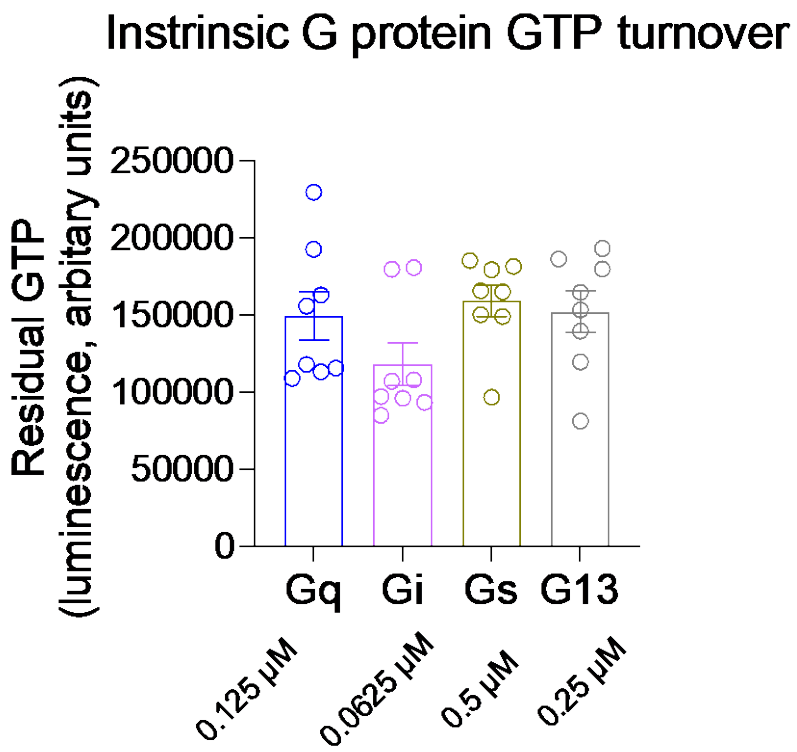

Supplemental Figure 4: Intrinsic G protein GTP hydrolysis in the absence of M_3R in the GTP-Glo™ assay. Concentrations of G protein in the absence of receptor were titrated to yield similar levels of baseline GTP turnover. In our measurements, the relative rank order of intrinsic GTP turnover was broadly assessed to be Gi>>Gq>G13>Gs over a 30-minute incubation timeframe. No statistically significant difference was observed between these conditions ($p>0.05$, one-way ANOVA; and for each pairwise comparison, $p>0.05$, Tukey's post-hoc multiple comparison analyses).

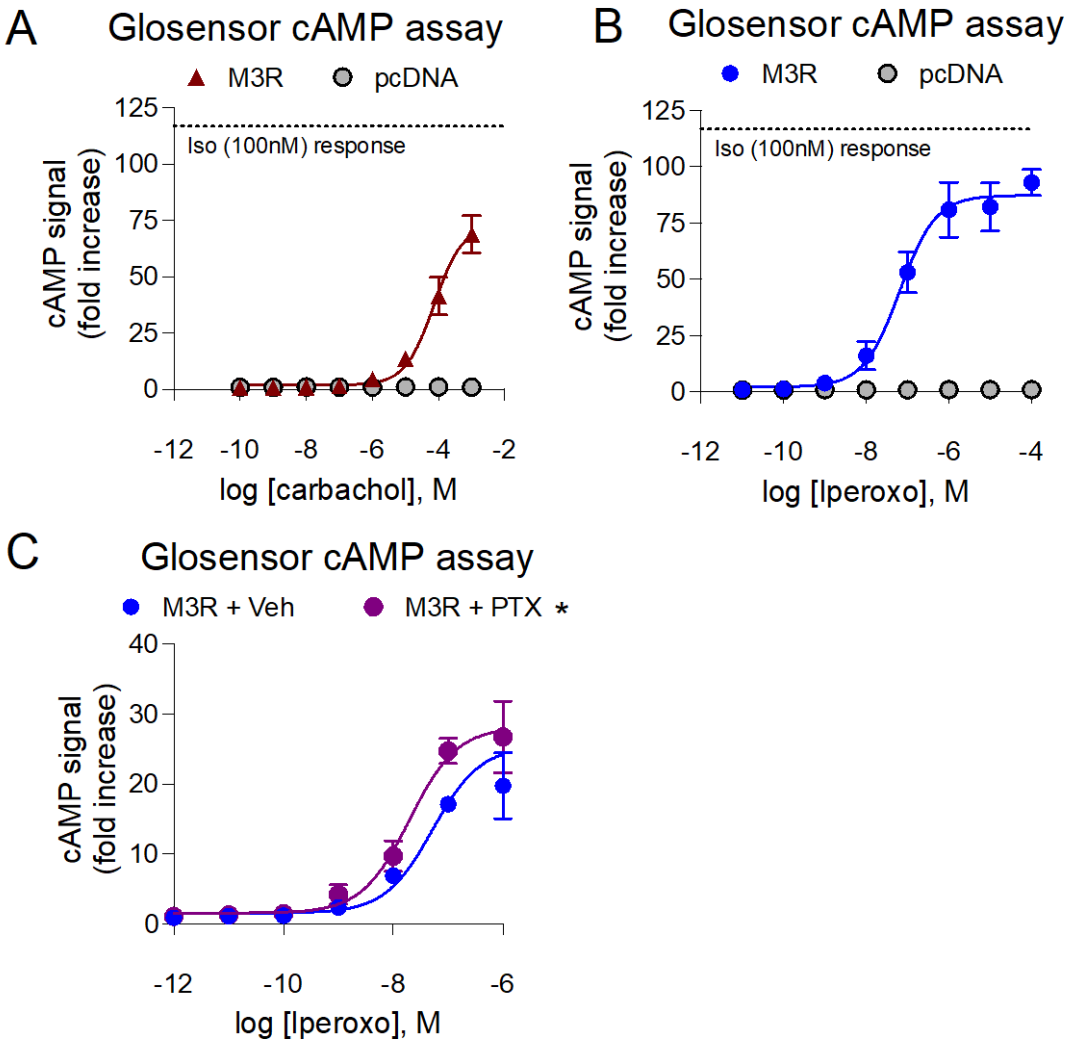

Supplemental Figure 5: Glosensor cAMP assay as an orthogonal measure of cellular cAMP levels. HEK 293T cells were transiently transfected with the Glosensor modified firefly luciferase and either M_3R or pcDNA empty vector control. Both (A) carbachol and (B) iperoxo increased luciferase signal in a dose-dependent manner. (C) PTX (200 ng/mL) pretreatment significantly increased cAMP signal. n=3 for panels A and B, n=2 for panel C. *, $p<0.05$, two-way ANOVA, main effect of PTX. PTX, pertussis toxin.

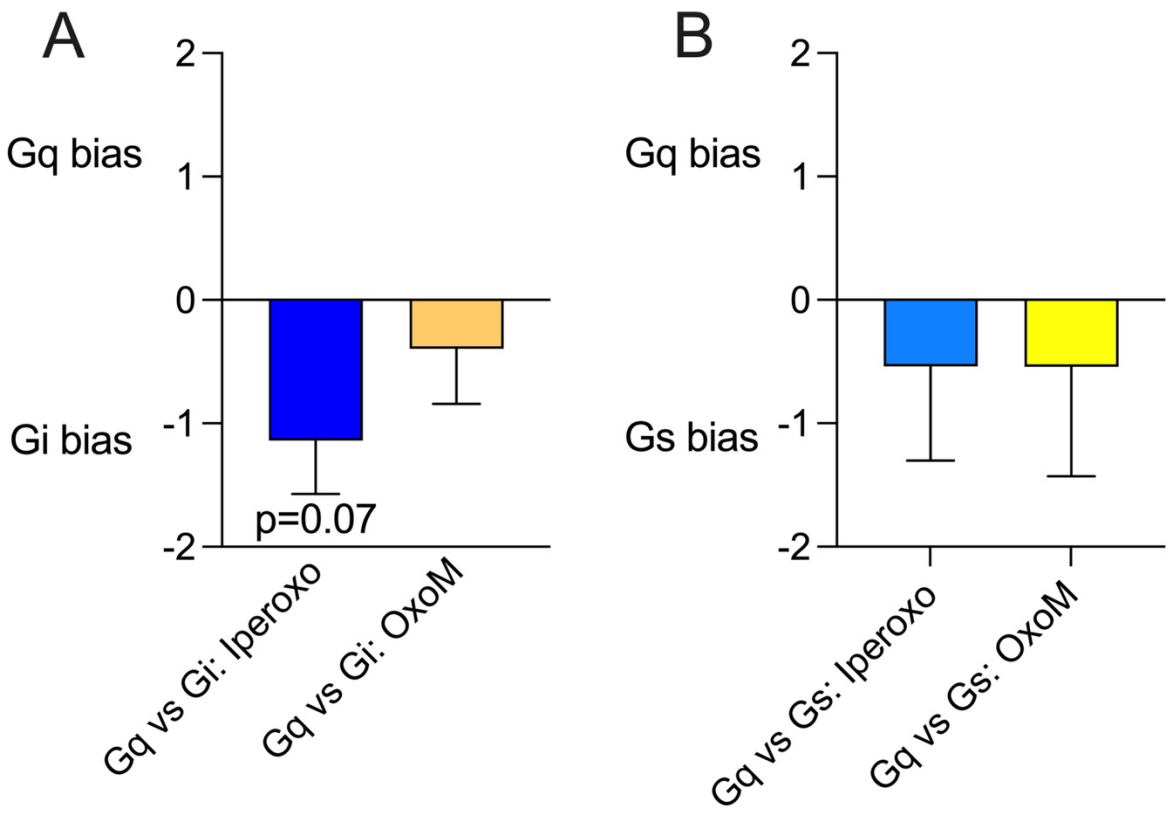

Supplemental Figure 6: Bias calculations of TRUPATH data comparing Gq vs Gi or Gs activity, using the intrinsic relative activity model (Smith, Lefkowitz and Rajagopal, 2018). Carbachol was used as the reference agonist. The rank order of EC_{50} did not change between ligands, but Gi bias relative to Gq for the agonist iperoxo was p=0.07 using a one sample, two-tailed t-test, with a bias factor of '0' taken as the null hypothesis, although this result was not statistically significant. OxoM, Oxotremorine-M.